Marine Chemistry 202 (2018) 49–57

Contents lists available at ScienceDirect

Marine Chemistry

journal homepage: www.elsevier.com/locate/marchem

# Kinetics of nitrous oxide production from hydroxylamine oxidation by birnessite in seawater

Amanda R. Cavazos*, Martial Taillefert, Yuanzhi Tang, Jennifer B. Glass*

*School of Earth and Atmospheric Sciences, Georgia Institute of Technology, Atlanta, GA, USA*

ARTICLE INFO

*Keywords:*
Nitrous oxide
Kinetics
Manganese oxides
Hydroxylamine

ABSTRACT

This study characterized the kinetics of abiotic production of the greenhouse gas nitrous oxide ($N_2O$) by chemical oxidation of the nitrification intermediate hydroxylamine ($NH_2OH$) in seawater at circumneutral pH (6.2–8.3). The oxidant was birnessite, a ubiquitous manganese oxide mineral in a variety of marine environments. Experiments using microsensor electrodes for high-resolution measurements of $N_2O$ production combined with the simultaneous measurements of the removal of $NH_2OH$ using spectrophotometric techniques revealed that the reaction was overall first order with the rate law $d[N_2O]/dt = k[NH_2OH]^{0.9}[MnO_2]^{0.3}[H^+]^0$ where $k$ is $0.01\ s^{-1}$. Birnessite consistently oxidized 80–100% of $NH_2OH$ to $N_2O$ within 3 min. Mass balance on nitrogen indicated rapid formation and disappearance of an intermediate species that was evidently involved in the formation of $N_2O$. In the presence of a nitroxyl (HNO) scavenger, $N_2O$ production rates and yield were suppressed by 17–59% and ~50%, respectively, suggesting that HNO is an intermediate in $NH_2OH$ oxidation to $N_2O$. These results support a mechanism whereby Mn(IV) is reduced to Mn(III) with the formation of an aminoxyl radical as the first product of $NH_2OH$ oxidation, which donates a second electron to another Mn(IV) center, or reduces the same Mn(III), to release $Mn^{2+}$ and HNO in solution. The final step is predicted to be HNO dimerization to $N_2O$ given the complete oxidation of $NH_2OH$ to $N_2O$ at steady-state. The experimentally-derived second-order rate constant for the dimerization step suggests that adsorption of HNO onto the excess solid surface controls the rate of $N_2O$ formation. Our findings suggest that abiotic $NH_2OH$ oxidation could be an important source of $N_2O$ in coastal ecosystems such as open oceans and oxygen minimum zones as well as sediment ecosystems wherever nitrification occurs in the presence of particulate metal oxides.

## 1. Introduction

Nitrous oxide ($N_2O$) is a potent greenhouse gas with over 250 times the warming potential of carbon dioxide per 100 year timescale (IPCC 2014). Bacterial nitrification ($NH_4^+ \rightarrow NH_2OH \rightarrow NO \rightarrow N_2O$), denitrification ($NO_3^- \rightarrow NO_2^- \rightarrow NO \rightarrow N_2O \rightarrow N_2$), and nitrifier denitrification ($NH_4^+ \rightarrow NH_2OH \rightarrow NO \rightarrow NO_2^- \rightarrow NO \rightarrow N_2O$) all contribute to global $N_2O$ emissions (Caranto and Lancaster 2017; Stein 2011), while archaeal nitrification may be an important source of $N_2O$ from the oceans (Santoro et al. 2011).

Recent studies have challenged the assumption that $N_2O$ is produced purely by enzymatic pathways, and highlighted the importance of understanding the mechanisms of coupled biotic-abiotic interactions between redox-active nitrogen and metal species (Kozlowski et al. 2016; Liu et al. 2017; Luther et al. 1997; Zhu-Barker et al. 2015). One such reaction is hydroxylamine ($NH_2OH$) oxidation coupled to the reduction of manganese (Mn) oxides such as $Mn(IV)O_2$:

$$2NH_2OH + 2Mn(IV)O_2 + 4H^+ \rightarrow N_2O + 2Mn^{2+} + 5H_2O \quad (1)$$

$\Delta G^{\circ\prime} = -106.2\ kJ\ mol\ e^{-1}$ (Zhu-Barker et al. 2015)

Hydroxylamine is an intermediate product of both aerobic and anaerobic microbial ammonia oxidation (Kartal et al. 2011; Oshiki et al. 2016; Vajrala et al. 2013; Yoshida and Alexander 1964). Birnessite (Mn(III, IV))$O_2$, hereafter referred to as $MnO_2$, is a ubiquitous Mn oxide mineral with a layered structure composed of $MnO_6$ octahedral sheets (Potter and Rossman 1979) and high redox potential (1.2 V; Zhou et al. 2006), and is capable of oxidizing a wide range of organic and inorganic species (Feng et al. 2015; Remucal and Ginder-Vogel 2014).

Although $NH_2OH$ oxidation by $MnO_2$ has been shown to contribute significantly to $N_2O$ emissions in terrestrial soils (Heil et al. 2015), this pathway has not been characterized in marine environments, which contributes to ~1/4 of global $N_2O$ emissions (Davidson and Kanter, 2014). Because Eq. (1) is thermodynamically favorable across a wide pH range (Luther 2010), it may occur when $NH_2OH$ that is leaked from nitrifying microbes encounters marine Mn oxides, such as in marine

* Corresponding authors.
*E-mail addresses:* acavazos3@gatech.edu (A.R. Cavazos), jennifer.glass@eas.gatech.edu (J.B. Glass).

https://doi.org/10.1016/j.marchem.2018.03.002
Received 11 January 2018; Received in revised form 12 March 2018; Accepted 13 March 2018
Available online 17 March 2018
0304-4203/ 

flocs suspended above oxyclines (Nameroff et al. 2002), at seawater-sediment interfaces (Lin and Taillefert 2014; Luther et al. 1997), and in ferromanganese nodules in deep sea sediments (Mallik 1980; Shiraishi et al. 2016). In this study, we characterized the kinetics of $NH_2OH$ oxidation by birnessite in synthetic seawater at circumneutral pH as a first step towards understanding the importance of abiotic $N_2O$ production in marine ecosystems.

## 2. Methods

### 2.1. Synthetic ocean water preparation

All chemicals used in the experiments were ACS grade or higher. All experiments were performed at pH above the $pK_a$ of $NH_2OH$ (5.9) to ensure that $NH_2OH$ was present in its unprotonated form. All glass and plastic ware were acid washed in 1.2 N HCl. Synthetic ocean water (SOW) was prepared according to Morel et al. (1979). Nitrogen and trace metal salts were excluded from the SOW, and pH was adjusted to 7.8 with KCl or KOH for all experiments except the variable pH experiments (see below).

### 2.2. Birnessite synthesis and characterization

Birnessite ($MnO_2$) was prepared according to Villalobos et al. (2003) and was equilibrated in SOW for 2–4 days prior to reaction with $NH_2OH$ (Bargar et al. 2005; Webb et al. 2005). A portion of the $MnO_2$ suspension was air-dried, finely ground, and analyzed by X-ray diffraction (XRD) using a PANalytical Empyrean diffractometer with Cu Kα source (initial scan range 10–85° with 0.0130 step size and 44.4 s step time), which confirmed the birnessite phase (Fig. S1). The concentration of Mn(III, IV) in the $MnO_2$-amended SOW (see below) was measured by the leucoberbelin blue colorimetric method (Krumbein and Altmann 1973) on an UV–Vis spectrophotometer (Genesys 20, Thermo Fischer Scientific).

### 2.3. $N_2O$ production measurement by microelectrode

Nitrous oxide production was measured with a $N_2O$ microsensor electrode and multimeter (Unisense, Aarhus, Denmark; 1 μM detection limit) while the solution was continuously stirred in 4.5 mL microrespiration chambers with lid ports. The microsensor was calibrated according to the manufacturer's protocol in $N_2O$ saturated solution in SOW (22 mM, using solubility constants from Weiss and Price (1980)) with $MnO_2$ concentrations corresponding to those in the experiments to correct for potential background noise due to particulates. All experiments were conducted in duplicate. Because $NH_2OH$ is highly reactive, all $NH_2OH$ solutions (as $NH_2OH{\cdot}HCl$, Sigma-Aldrich) were prepared in SOW within 10 min of use. Experiments were initiated by injecting $NH_2OH$ solution into the microrespiration chamber containing SOW with varied concentrations of $MnO_2$. Nitrous oxide concentrations were quantified every second for ~3 min. The isolation method was used to determine the order of the reaction with respect to each reactant, and all experiments were performed with excess oxidant ($MnO_2$; 300–1000 μM). Initial rates were determined by calculating the slope of $N_2O$ production over the first minute of the reaction using the least squares fit in MatLab (R2015a).

To test whether nitroxyl (HNO) was a reaction intermediate for Eq. (1), we performed another set of experiments in which the HNO scavenger *N*-acetyl-L-cysteine (Sigma-Aldrich) was added to the microrespiration chamber at 3× the $NH_2OH$ concentration. Despite its reactivity towards the $NO_2$ radical and peroxynitrite, *N*-acetyl-L-cysteine is as an effective HNO scavenger. *N*-acetyl-L-cysteine donates a thiol group (RSH) to HNO to form a thiol-bound HNO adduct (Samuni et al. 2013), effectively preventing dimerization to $N_2O$, though *N*-acetyl-L-cysteine may also react with the adduct to form $NH_2OH$ as by-product and ultimately enhance formation of $N_2O$ (Samuni et al. 2013). We also performed control experiments with $NH_4^+$ in place of $NH_2OH$ to determine if $N_2O$ was produced from oxidation of $NH_4^+$, a possible $NH_2OH$ decomposition product.

### 2.4. $NH_2OH$ consumption measurement by spectrophotometry

A parallel set of experiments were performed in 2.0 mL Eppendorf tubes to quantify $NH_2OH$ consumption and potential production of other dissolved N species. Hydroxylamine (100 μM) was added to SOW containing 0, 300, or 1000 μM $MnO_2$. Samples were collected every 5–30 s for 3 min and filtered through 0.45 μm cellulose acetate syringe filters (VWR International). Nitrate ($NO_3^-$) and nitrite ($NO_2^-$) concentrations were analyzed using the modified Griess method (García-Rodledo et al. 2014). Measurement of $NH_4^+$ by the phenol hypochlorite method (Solórzano 1969) was infeasible due the $NH_2OH$ interference (Riley 1953).

A variety of $NH_2OH$ spectrophotometric analyses were tested to determine the optimal procedure for our experimental conditions. When used with SOW, the reagents in the quinolinol method developed by Frear and Burrell (1955) formed a thick, cloudy precipitate, preventing further use. Instead, we optimized the iodine method, originally described by Fiadeiro et al. (1967) and improved in Strickland and Parsons (1972), for use in small volumes of SOW. Specifically, 1 mL sample was placed in a 2.0 mL Eppendorf tube, and 40 μL of sulphanilic acid and 20 μL iodine solution were added and allowed to react for 3 min. Then, 20 μL of a sodium arsenite solution was added and allowed to react for 2 min. Finally, 20 μL of *N*-(1-Napthyl)-ethylenediamine was added, color was allowed to develop for 15 min, and the absorbance at 543 nm was read by an UV–Vis spectrophotometer. Calibration curves were made using filtered $MnO_2$ solutions in SOW with a 0.45 μm cellulose acetate syringe filter to account for possible interferences from Mn.

## 3. Results

### 3.1. Mass balance

To determine the percent of $NH_2OH$ oxidized to $N_2O$ as a function of $MnO_2$ concentration, we quantified the consumption of $NH_2OH$ (initial concentration 100 μM) and production of $N_2O$ at pH 7.8. No detectable $NH_2OH$ consumption, and no more than 6 μM $N_2O$ (10% yield) production was observed in the absence of $MnO_2$ (Fig. 1a). In the presence of $MnO_2$, ≥50% $NH_2OH$ was consumed within 5 s of $NH_2OH$ addition, and 97–100% $NH_2OH$ was consumed within 210 s, exhibiting a pseudo-first order decay with a half-life of 20–25 s (Fig. 1b–f; Table 1). $NO_x^-$ production was minimal in all experiments (< 5 μM; data not shown). Mass balance indicates that an unknown intermediate species is produced initially, but then consumed over time (Fig. 1b–f). After accounting for the 2:1 substrate-to-product ratio, we found that 89–100% of $NH_2OH$ was converted to $N_2O$ at steady-state (Table 1), and that $N_2O$ yield from $NH_2OH$ was inversely proportional to the initial $NH_2OH$ concentration (Tables 1, 2). When HNO scavenger *N*-acetyl-L-cysteine was added, $N_2O$ production rates decreased by 17–59% (Fig. 2) while $N_2O$ production yields decreased by 41–52% (not shown). Minimal $N_2O$ was produced when $NH_2OH$ was replaced with $NH_4^+$ (Fig. 2).

### 3.2. Kinetic experiments to determine the overall order of the reaction and the rate constant

To determine the overall order and rate constant of the reaction, a general rate law for $NH_2OH$ oxidation by $MnO_2$ was developed:

$$\frac{d[NH_2OH]}{dt} = -k[NH_2OH]^a[MnO_2]^b[H^+]^c \quad (2)$$

where *a*, *b*, and *c* represent the order of the reaction with respect to each reactant, and *k* is the rate constant.

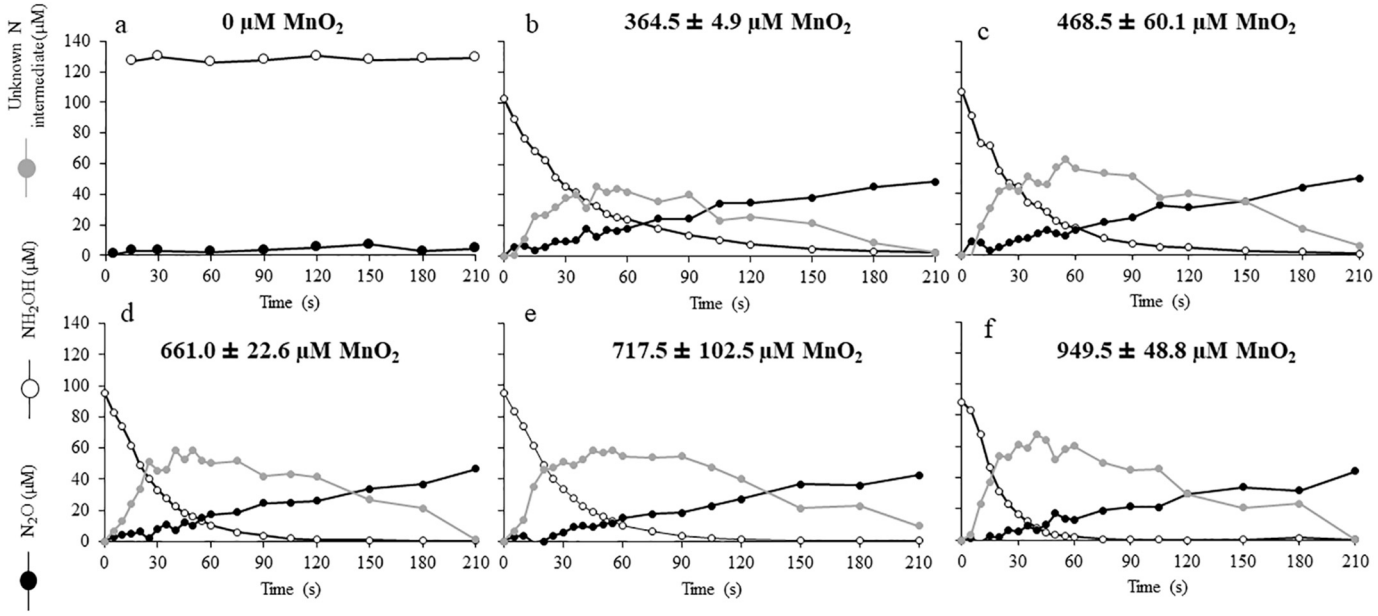


**Fig. 1.** Complete conversion of $NH_2OH$ to $N_2O$ in various experiments. Mass balance conserved between $NH_2OH$ and $N_2O$ from experiments conducted with 100 μM $NH_2OH$ with varied concentrations of $MnO_2$ at pH 7.8. Conversion to $N_2O$ ranged from 89 to 100%.

### 3.2.1. Order with respect to $NH_2OH$

To determine the order with respect to $NH_2OH$, the isolation method was used, in which initial $NH_2OH$ concentrations were varied while $MnO_2$ and pH were kept constant, such that Eq. (2) can be re-arranged to give:

$$\frac{d[NH_2OH]}{dt} = -k_{obs}[NH_2OH]^a \quad (3)$$

where

$$k_{obs} = k[MnO_2]^b[H^+]^c \quad (4)$$

If the unknown intermediate species is rapidly produced and consumed, the steady-state hypothesis can be used to relate the rate of $NH_2OH$ consumption to the rate of $N_2O$ production measured by the microsensor such that Eq. (3) becomes:

$$-\frac{d[NH_2OH]}{dt} = 2\frac{d[N_2O]}{dt} = R = k_{obs}[NH_2OH]^a \quad (5)$$

where $R$ is twice the rate of $N_2O$ production. As the rate of $N_2O$ production was linear over most of the reaction (Fig. 3a), it was possible to use the initial rate method to obtain $a$ after rearranging Eq. (5) to:

$$\log(R) = \log(k_{obs}) + a \times \log([NH_2OH^\circ]) \quad (6)$$

where $[NH_2OH^\circ]$ is the initial concentration of $NH_2OH$.

We found that initial $N_2O$ production rates increased linearly with increasing $NH_2OH$ concentrations (Fig. 3a). The slope of Eq. (6) gives $a$, the order of reaction with respect to $NH_2OH$, which was found to be first order ($a = 0.9 \pm 0.07$; Fig. 4a).

### 3.2.2. Order with respect to $MnO_2$

To determine the order of the reaction with respect to $MnO_2$, experiments were performed by injecting 100 μM $NH_2OH$ into 361, 414, 426, 677, and 915 μM $MnO_2$ at pH 7.8 and monitoring $NH_2OH$ concentrations as a function of time (Fig. 1b–f). Because the order of the reaction with respect to $NH_2OH$ was ~1 (Fig. 4a), Eq. (2) can be re-arranged to:

$$\frac{d[NH_2OH]}{dt} = k_{obs}[NH_2OH] \quad (7)$$

where

$$k_{obs} = k[MnO_2]^b[H^+]^c \quad (8)$$

In this case, the initial rate method was used to calculate the $k_{obs}$ from Eq. (7) for each experiment. The order of the reaction, $b$, was then determined from the linearized form of Eq. (8) by representing $\log k_{obs}$ at each concentration of $MnO_2$ as a function of the initial concentration of $MnO_2$ at fixed pH:

$$\log(k_{obs}) = \log(k[H^+]^c) + b \times \log[MnO_2] \quad (9)$$

Using this approach, a slope *(b)* equal to the order of reaction with respect to $MnO_2$, of 0.3 ± 0.08, was found (Fig. 4b).

### 3.2.3. Order with respect to proton concentration

To determine the order of reaction with respect to the proton concentration, experiments were carried out by injecting 100 μM $NH_2OH$ into 300 μM $MnO_2$ at pH 6.2, 6.7, 7.0, 7.8, and 8.3, and monitoring $N_2O$ concentrations as a function of time (Fig. 3c). The same method used for determining the order of reaction with respect to $MnO_2$ was used for determining the order of reaction with respect to the proton

**Table 1**
Mass balance between $NH_2OH$ and $N_2O$ from the varied $MnO_2$ experiments. All values represent an average value ($n = 2$).

| $[MnO_2]$ (μM) | $[NH_2OH^\circ]$ (μM) | $[NH_2OH_f]$ (μM) | $[N_2O]$ (μM) | % $NH_2OH$ consumption | % $NH_2OH$ conversion to $N_2O$ |
|---|---|---|---|---|---|
| 364.5 ± 4.9 | 103.0 ± 16.7 | 2.6 ± 1.0 | 48.8 ± 5.4 | 97.5 | 97.2 |
| 468.5 ± 60.1 | 107.3 ± 1.7 | 0.8 ± 0.2 | 50.2 ± 0.2 | 99.3 | 94.3 |
| 661.0 ± 22.6 | 95.5 | 0.4 ± 0.2 | 46.9 ± 9.1 | 99.6 | 98.6 |
| 717.5 ± 102.5 | 95.5 | 0.4 ± 0.2 | 42.5 ± 6.5 | 99.6 | 89.4 |
| 949.5 ± 48.8 | 88.6 ± 1.7 | 0.3 ± 0.3 | 44.0 ± 13.1 | 99.7 | 99.7 |

**Table 2**
Nitrous oxide production rates, rate constants, $k$, and maximum $N_2O$ yield of each experimental condition for each duplicate. Rate constant is first order.

| [$MnO_2$] ($\times 10^{-6}$ M) | [$NH_2OH$] ($\times 10^{-6}$ M) | pH | $Rate_{N2O}$ (D1) ($\times 10^{-7}$ M $s^{-1}$) | $Rate_{N2O}$ (D2) ($\times 10^{-7}$ M $s^{-1}$) | $k_{N2O}$ (D1) ($\times 10^{-3}$ $s^{-1}$) | $k_{N2O}$ (D2) ($\times 10^{-3}$ $s^{-1}$) | $Rate_{NH2OH}$ (D1) ($\times 10^{-7}$ M $s^{-1}$) | $Rate_{NH2OH}$ (D2) ($\times 10^{-7}$ M $s^{-1}$) | $k_{NH2OH}$ (D1) ($\times 10^{-3}$ $s^{-1}$) | $k_{NH2OH}$ (D2) ($\times 10^{-3}$ $s^{-1}$) | Mean yield (%) |
|---|---|---|---|---|---|---|---|---|---|---|---|
| 790 | 100 | 7.8 | 2.40 | 2.02 | 8.14 | 6.85 | | | | | 91.3 |
| | 150 | | 3.21 | 3.08 | 7.57 | 7.25 | | | | | 82.5 |
| | 200 | | 3.58 | 3.86 | 6.52 | 7.03 | | | | | 80.4 |
| | 250 | | 4.96 | 5.26 | 7.38 | 7.82 | | | | | 80.1 |
| | 300 | | 6.05 | 6.08 | 7.64 | 7.68 | | | | | 79.7 |
| | | | | | **7.45 ± 0.59** | **7.33 ± 0.42** | | | | | |
| 361 | 100 | 7.8 | 2.20 | 2.40 | 9.45 | 10.3 | 3.34 | 4.65 | 13.9 | 19.3 | 100 |
| 414 | | | 1.95 | 2.35 | 8.02 | 9.70 | 3.59 | 4.49 | 13.0 | 16.3 | 92.1 |
| 426 | | | 2.06 | 2.43 | 8.43 | 9.94 | 2.87 | 4.21 | 10.8 | 15.8 | 96.9 |
| 677 | | | 1.92 | 2.11 | 6.82 | 7.39 | 2.84 | 3.17 | 10.1 | 11.2 | 90.5 |
| 915 | | | 1.76 | 2.16 | 5.71 | 7.01 | 2.55 | 2.51 | 9.1 | 9.0 | 92.7 |
| | | | | | **7.69 ± 1.45** | **8.89 ± 1.52** | | | | | |
| 300 | 100 | 6.2 | 2.14 | 2.21 | 10.1 | 10.5 | | | | | 100 |
| | | 6.7 | 1.99 | 2.33 | 9.13 | 10.7 | | | | | 100 |
| | | 7.0 | 2.36 | 2.26 | 10.9 | 10.5 | | | | | 96.9 |
| | | 7.8 | 2.18 | 2.45 | 9.73 | 10.9 | | | | | 100 |
| | | 8.3 | 2.59 | 2.28 | 11.3 | 9.94 | | | | | 100 |
| | | | | | **10.2 ± 0.87** | **10.5 ± 0.37** | | | | | |
| | | | | | **8.68 ± 1.60** | | | | **12.9 ± 3.5** | | |

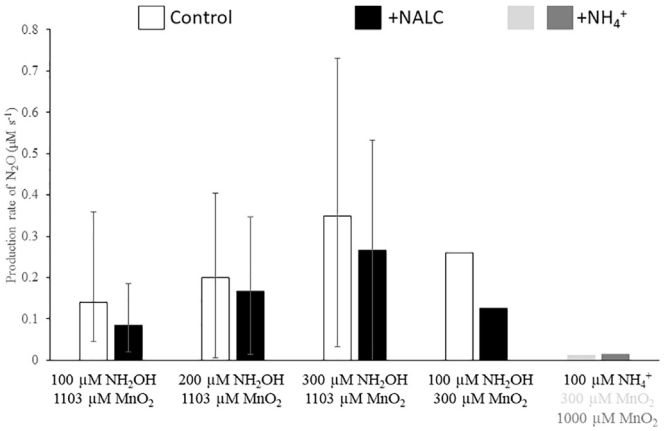


**Fig. 2.** Addition of *N*-acetyl-L-cysteine decreases $N_2O$ production rates, and there is no noticeable $N_2O$ production from $NH_4^+$. Nitrous oxide production rates decrease with 300–900 μM *N*-acetyl-L-cysteine addition (3× $NH_2OH$ concentration) at pH 7.8. Error bars, when present, show range of data ($n$ = 2, except for 100 μM $NH_2OH$ into 1103 μM $MnO_2$ where $n$ = 3). No error bars represent single experiments ($n$ = 1).

concentration. The slope of the initial rate of $N_2O$ production represented as a function of the initial concentration of $NH_2OH$ (Eq. 7) was used to calculate the pseudo-first order rate constant ($k_{obs}$) at each pH. The order of the reaction with respect to proton concentration, $c$, was then determined by linearizing Eq. (8) to:

$$\log k_{obs} = \log([kMnO_2]^b) + c \times \log[H^+] \quad (10)$$

The slope of the log of the $k_{obs}$ as a function of the pH (Eq. (10)) indicates a zero order reaction with respect to pH ($c$ = 0.007 ± 0.011) at circumneutral pH (Fig. 4c).

### 3.2.4. Rate law

The orders of each reactant were substituted into Eq. (2) to give Eq. (11):

$$\frac{dN_2O}{dt} = k\,[NH_2OH]^{0.9}\,[MnO_2]^{0.3} \quad (11)$$

When the production rates of $N_2O$ and initial concentrations of $NH_2OH$ and $MnO_2$ from each experiment (Table 2) are substituted into Eq. (11), the overall first order rate constant, $k$, is found to be 0.009 ± 0.002 $s^{-1}$. When the overall first order rate constant is calculated using $NH_2OH$ oxidation rates, $k$ is found to be

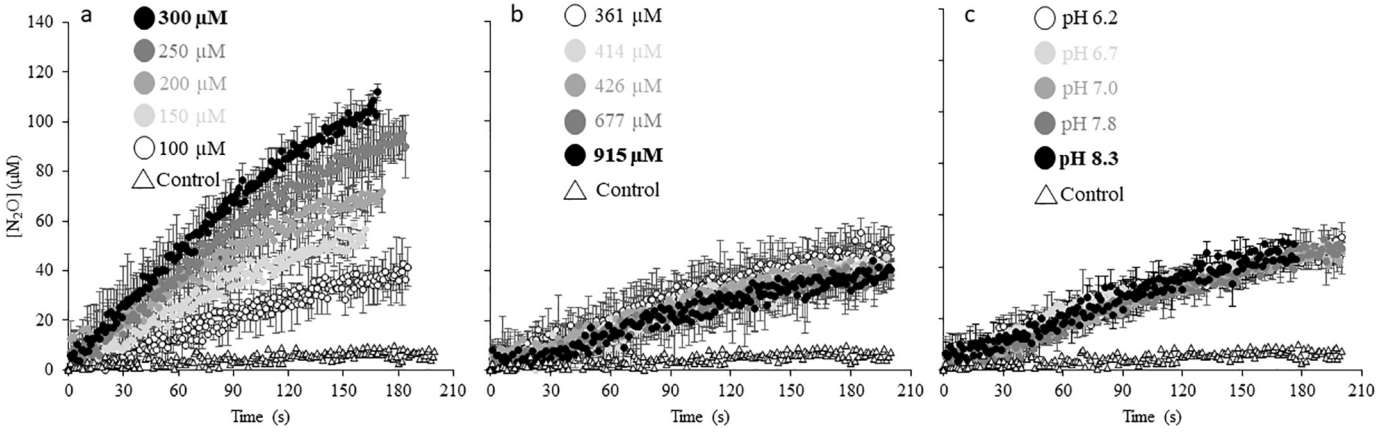


**Fig. 3.** Nitrous oxide production rates increase with increasing $NH_2OH$. Averaged $N_2O$ production rate from (a) varied initial $NH_2OH$ concentrations into 790 μM $MnO_2$ at pH 7.8 ± 0.1, (b) 100 μM $NH_2OH$ into varied initial $MnO_2$ concentrations at pH 7.8 ± 0.1, and (c) 100 μM $NH_2OH$ into 300 μM $MnO_2$ at varied but constant pH. The control (open triangles) represents 100 μM $NH_2OH$ into SOW with no $MnO_2$. Slope and standard error of the averaged best fit line ($n$ = 2) are shown below varied parameters.

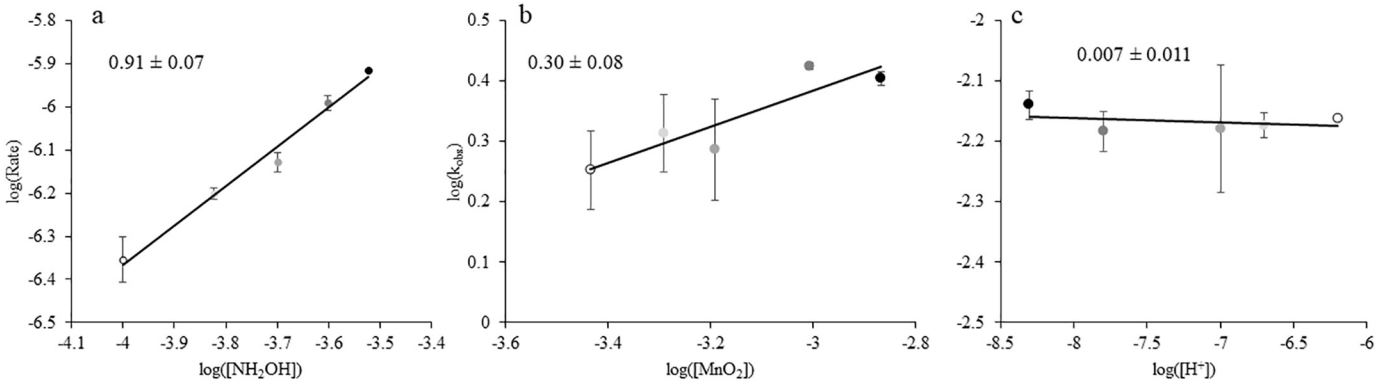


**Fig. 4.** The order of reaction with respect to (a) $NH_2OH$, (b) $MnO_2$, and (c) pH. Data points represent the average of the duplicates, and error bars represent standard deviation between the duplicates. Calculations of $k_{obs}$ are described in Section 2.2 of the text.

$0.013 \pm 0.004\,s^{-1}$. The good agreement between these two calculations indicates that the steady-state hypothesis used to calculate the order of the reaction with respect to $NH_2OH$ and proton concentrations was appropriate.

## 4. Discussion

### 4.1. Mineral effects on $NH_2OH$ reactivity

To our knowledge, this is the first study that measures the kinetics of $NH_2OH$ oxidation by an environmentally-relevant mineral substrate ($MnO_2$). In previous studies with enzyme-bound Mn(IV) or ligand-bound Mn(III) in pure water or acidic perchlorate solution (Table 3), $NH_2OH$ was suggested to interact with the Mn(III, IV) center by outer-sphere complexation (Banerjee et al. 2002; Salem 1995). In this study, $NH_2OH$ oxidation takes place at the $MnO_2$ mineral surface, where high surface area, small particle size, and highly reactive surface sites mediate rapid reaction. In seawater, abundant cations may enter the interlayer region of birnessite and replace water molecules, leading to strong aggregation (Holland and Walker 1996; Villalobos et al. 2003). Thus, the small decrease in $N_2O$ production rates observed at increasing $MnO_2$ concentration (Table 2) may be due to aggregation.

### 4.2. Known competing reactions

We considered the following abiotic processes to explain the findings reported above.

#### 4.2.1. Nitrosation

Nitrosation involves the transfer of a NO group from nitrous acid compound to a nitrogenous nucleophilic center. For example, $NH_2OH$ and HNO can react to form $N_2$:

$$HNO + NH_2OH \rightarrow N_2 + 2H_2O \quad (12)$$

$\Delta G_r^\circ = -328.78\,kJ\,mol\,e^{-1}$ (Latimer 1952; Shafirovich and Lymar 2002).

At low pH, $NH_2OH$ may be oxidized by $HNO_2$ to form $N_2O$ (Hussain et al. 1968; Soler-Jofra et al. 2016):

$$NH_2OH + HNO_2 \rightarrow N_2O + 2H_2O \quad (13)$$

$$NH_3OH^+ + HNO_2 \rightarrow N_2O + H_2O + H_3O^+ \quad (14)$$

Nitroxyl (HNO) may also dimerize to produce $N_2O$:

$$HNO + HNO \rightarrow N_2O + H_2O \quad (15)$$

The importance of Eq. (12) has been demonstrated at high $NH_2OH$:$Na_2N_2O_3$ (HNO donor) ratios and may explain the lower $N_2O$ yields with high $NH_2OH$ (Table 2), but the reaction is slower than HNO dimerization (Eq. (15); Fehling and Friedrichs 2011; Shafirovich and Lymar 2002), and is unlikely to be important in natural waters with low $NH_2OH$ (see below). Eqs. (13) and (14) are unlikely to have occurred in this study because all experiments were performed above the $pK_a$ of $NH_2OH$ (5.9) and $HNO_2$ (2.8), and $NO_2^-$ concentrations did not significantly change during the reaction (data not shown). Together with the fact that the addition of a HNO scavenger decreased rates (Fig. 2) and yields (not shown) of $N_2O$ production, these considerations suggest that HNO dimerization is the most likely nitrosation reaction to occur in these experiments.

#### 4.2.2. Hydroxylamine disproportionation

Hydroxylamine disproportionation (or autoxidation) to $NH_4^+$, $N_2O$ or $N_2$ (Bari et al. 2010; Bonner et al. 1978) is described by the following reactions:

$$2NH_2OH + H^+ \rightarrow NH_4^+ + HNO + 3H_2O \quad (16)$$

$$4NH_2OH + 2H^+ \rightarrow N_2O + 2NH_4^+ + 3H_2O \quad (17)$$

$$3NH_2OH + H^+ \rightarrow N_2 + NH_4^+ + 3H_2O \quad (18)$$

These reactions are catalyzed by copper and other reduced metals (Anderson 1964; Butler and Gordon 1986; Moews Jr and Audrieth, 1959). Hydroxylamine disproportionation was ruled out in the present system because $NH_2OH$ levels remained constant in the absence of $MnO_2$, with only background levels of $N_2O$ present (Fig. 1a). While $NH_4^+$ can be oxidized to $NO_3^-$ or $NO_2^-$ by $MnO_2$ at environmentally relevant pH, mM levels of $NH_4^+$ are required to produce $< 10\,\mu M$ $NO_3^-$ or $< 100\,\mu M$ $NO_2^-$ (Boumaiza et al. 2018).

#### 4.2.3. Nitrous oxide reduction by $Mn^{2+}$

The reduction of $N_2O$ by $Mn^{2+}$ was considered a possible mechanism for a general decrease in $N_2O$ production rates with increasing $MnO_2$ concentrations (Figs. 3b; Table 2). In the investigated reaction (Eq. 1), $Mn^{2+}$ would be produced simultaneously with $N_2O$, and this $Mn^{2+}$ could, in theory, reduce $N_2O$ to $N_2$:

$$N_2O + Mn^{2+} + H_2O \rightarrow N_2 + MnO_2 + 2H^+ \quad (19)$$

$\Delta G^\circ = -52.06\,kJ\,mol\,e^{-1}$

Eq. (19) could account for the small fraction of missing N in our mass balance. If $N_2$ produced by this reaction was the missing nitrogen fraction, however, it should have increased as a function of time, as $Mn^{2+}$ was progressively produced during the reduction of $MnO_2$ by $NH_2OH$. As the missing nitrogen fraction was immediately produced and progressively removed from solution (Fig. 1), this reaction was likely not significant in these experiments.

#### 4.2.4. Nitroxyl binding by $Mn^{3+}$

A more likely explanation for the increased rates of $NH_2OH$ consumption with increasing $MnO_2$, without significant change in rates of

**Table 3**
Comparison of $NH_2OH$ oxidation by a variety of Mn species and other relevant reactions under various experimental conditions.

| $NH_2OH$ oxidation and other reactions | Solution | Measurement method | pH | Overall order | Rate constant | Source |
|---|---|---|---|---|---|---|
| Tri-bridged Mn(IV,IV) dimer | Double-distilled water | Spectrophotometry | 4.0–5.3 | 1 | $2.0–15.0 \times 10^{3}\ s^{-1}$ | Banerjee et al. (2002) |
| Mn(III) | Acidic perchlorate media | Spectrophotometry | 0.5-0.2 | 2 | $1.5–2.7 \times 10^{-3}\ M^{-1}\ s^{-1}$ | Davies and Kustin (1969) |
| Bis(pentane-2,4-dionato)diaquo manganese(III) | Double-distilled water | Spectrophotometry/titration | 5.02–5.70 | 1 | $6.65–158\ s^{-1}$ | Hynes et al. (1993) |
| Mn(III)-bis(salicylaldimine) complexes | Double-distilled water | Spectrophotometry | 5.2–8.4 | 2 | $0.16–7.44\ M^{-1}\ s^{-1}$ | Salem (1995) |
| Acid birnessite ($MnO_2$) | Synthetic ocean water | Microsensor/spectrophotometry | 6.2–8.3 | 1 | $4.09 \pm 0.33 \times 10^{-4}\ s^{-1}$ | This study |
| HNO dimerization | Milli-Q purified water | UV steady-state photolysis | 11–14.3 | 2 | $8 \pm 3 \times 10^{6}\ M^{-1}\ s^{-1}$ | Shafirovich and Lymar (2002) |
| HNO reduction by $NH_2OH$ | Deionized water with chelator | Spectrophotometry/computational | 7.45 | 2 | $4.0 \pm 0.3 \times 10^{-7}\ M^{-1}\ s^{-1}$ | Jackson et al. (2009) |
| HNO trapping by ligand-bound $Mn^{3+}$ center | 0.1 M phosphate buffer with EDTA | Spectroscopy | 7 or 10 | 2 | $4–9 \times 10^{4}\ M^{-1}\ s^{-1}$ | Martí et al. (2005) |

$N_2O$ production (Figs. 1, 3b), may be trapping of the intermediate HNO by mineral-bound Mn(III). Such HNO trapping has been observed using porphyrin-bound $Mn^{3+}$ in solution (Martí et al. 2005). The suppression of $N_2O$ production by the HNO scavenger (Fig. 2) suggests that HNO was likely an intermediate in the oxidation of $NH_2OH$ by $MnO_2$ (Eq. (1)). If mineral-bound Mn(III) was present or formed during the reaction, it could bind the HNO intermediate at the mineral surface, thereby preventing HNO dimerization to $N_2O$ (Eq. (15)). This pathway requires formation of an aminoxyl radical (Banerjee et al. 2002; Davies and Kustin 1969; Salem 1995) that may further reduce a Mn(IV) metal center to Mn(III), and either scavenge HNO, or reduce the same Mn(III) intermediate to release both $Mn^{2+}$ and HNO into solution. Release of HNO to solution is likely followed by dimerization to $N_2O$. Although these mechanistic details will be difficult to distinguish experimentally, the high $N_2O$ yield at steady-state (Tables 1 and 2) indicates the sequestration of HNO onto the solid phase was likely not significant.

### *4.3. Proposed reaction sequence and mechanisms of $NH_2OH$ oxidation to $N_2O$ by $MnO_2$*

Here we propose a reaction sequence for the oxidation of $NH_2OH$ to $N_2O$ by $MnO_2$ consistent with our experimental findings and mass balance. Birnessite is well known to have low zero point charge (e.g. ~2.25; Balistrieri and Murray 1982; Murray 1974), making the surface charge negative across a wide range of pH, including the circumneutral pH values used in this study. This surface property, combined with its high surface area and presence of structural vacancy sites, makes birnessite highly reactive for the sorption of various species, especially positively charged species such as metal cations. The lone electron pair on N in $NH_2OH$ is likely to introduce a polar effect; thus, the molecule can be attracted to charged surfaces such as the birnessite surface. Although the exact location (e.g. vacancy site vs. edge site) and mechanism (e.g. inner-sphere vs. outer-sphere) of the interaction is unclear, $NH_2OH$ as a polar molecule can possibly form an adsorbed complex with the birnessite surface, transferring an electron to a Mn (IV) atom (Fig. 5a), reducing Mn(IV) to Mn(III), and also resulting in the deprotonation of the hydroxyl group that forms the aminoxyl radical ($H_2NO\cdot$) (Fig. 5a). The electron from the $H_2NO\cdot$ radical can be further transferred to either the produced Mn(III) to yield HNO and dissolved Mn(II) (Fig. 5b), or to another Mn(IV) atom to produce another Mn(III) and adsorbed HNO surface complex (Fig. 5c). The HNO species produced by these two reactions likely represents the transient nitrogen intermediate species derived from mass balance calculations (Fig. 1). As proposed by Fehling and Friedrichs (2011), HNO dimerizes to form *cis*-ON(H)N(H)O, which readily deprotonates to form *cis*-$ONN(H)O^-$ (Fig. 5d) and rearranges to the protonated *cis*-HONN(O)H at circumneutral pH (Fig. 5e). Deprotonation of this intermediate forms the poorly stable *cis*-hyponitrite anion ($HONNO^-$; Fig. 5e), which loses a hydroxyl group to form $N_2O$ and water at circumneutral pH (Fig. 5f). Considering that the HNO intermediate is completely removed by the end of the reaction (Fig. 1), it is possible to estimate the pseudo-second order rate constant of its removal by dimerization by representing the linear form of the integrated equation after the time of its maximum production (Fig. 6). The rate constant of HNO dimerization to $N_2O$, $k_2$, is found to be $239 \pm 93\ M^{-1}\ s^{-1}$, significantly lower than that presented by Shafirovich and Lymar (2002) ($8 \times 10^{6}\ M^{-1}\ s^{-1}$), though their experiments were conducted at much higher pH than reported here. Adsorption of HNO on the excess $MnO_2$ used in these experiments may also be responsible for the decline in the rate of HNO dimerization. As $NH_2OH$ consumption rates increased slightly at increasing $MnO_2$ concentration, while no discernible change in $N_2O$ production rates were observed, it is likely that the rate-limiting step occurs after the initial electron transfer. The good reproducibility of the dimerization kinetic data at varying $MnO_2$ concentrations (Fig. 6) suggests that the dimerization of HNO may be the rate-limiting step and controlled by the adsorption of HNO onto the $MnO_2$ surface.

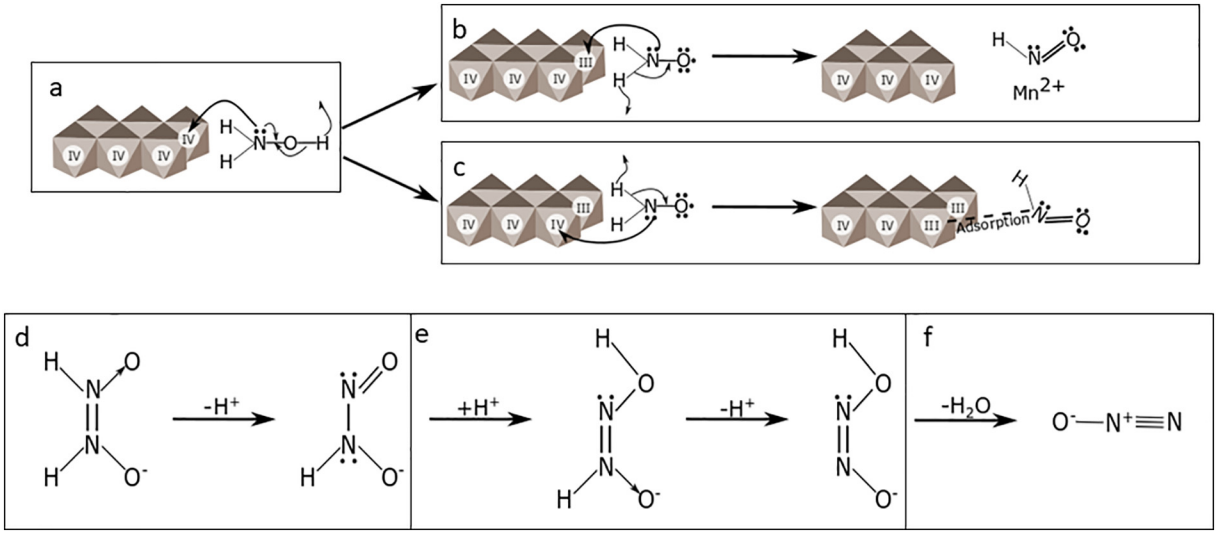


**Fig. 5.** Proposed mechanism for $NH_2OH$ oxidation by birnessite. (a) Electron transfer from $NH_2OH$ to the Mn(IV) and deprotonation of the hydroxyl group allow formation the aminoxyl radical ($H_2NO\cdot$) and reduction of the Mn(IV) to Mn(III). The electron from the $H_2NO\cdot$ is transferred to either (b) the Mn(III) to produce nitroxyl (HNO) and $Mn^{2+}$ or (c) to another Mn(IV) to produce another Mn(III) and HNO which then could adsorb onto the Mn(III) product. (d) Nitroxyl dimerizes to form *cis*-ON(H)N(H)O, which deprotonates to *cis*-ON(H)$NO^-$. (e) O-protonation occurs and forms *cis*-HONN(O)H, which deprotonates to the unstable *cis*-hyponitrite anion ($HONNO^-$). (f) The *cis*-hyponitrite anion loses its hydroxyl group to form $N_2O$.

### 4.4. Environmental implications

Based on our findings, rapid $N_2O$ production from the coupled biotic-abiotic reaction of microbial $NH_4^+$ oxidation to $NH_2OH$, followed by abiotic $NH_2OH$ oxidation by Mn(III, IV) oxides, could occur wherever active nitrifying and $Mn^{2+}$-oxidizing bacteria coexist (Clement et al. 2009; Tebo 1991). Relevant environments include oxyclines above oxygen minimum zones (Beman et al. 2012; Bouskill et al. 2012; Bruland et al. 1994; Löscher et al. 2012; Neretin et al. 2003; Newell et al. 2011; Shiller and Gieskes 1985; Trefry et al. 1984), sediment-water interfaces (Anschutz et al. 2005), and deep sea sediments that contain ferromanganese nodules (Blöthe et al. 2015; Shiraishi et al. 2016). In oceanic environments, particulate Mn tends to be low in concentration, which would decrease the likelihood of aggregation, and potentially lead to faster rates of $N_2O$ production than observed in our experiments.

Hydroxylamine is likely the limiting substrate for Eq. (1) in nature because $NH_2OH$ occurs at low concentrations and is an essential intermediate in nitrification. During periods of intense nitrification in coastal waters, $NH_2OH$ can accumulate up to ~200 nM (Butler et al. 1987, 1988; Gebhardt et al. 2004; Schweiger et al. 2007). The presence of $NH_2OH$ in natural waters indicates that it leaks out of cells, and suggests that the fast $N_2O$ production from abiotic $NH_2OH$ oxidation with Mn(III/IV) oxides could be easily confused with $N_2O$ from biological nitrification (Kozlowski et al. 2016). Using representative conservative concentrations from the oxycline Baltic Sea, 31 nM $MnO_2$ (Neretin et al. 2003) and 18 nM $NH_2OH$ (Schweiger et al. 2007) and Eq. (11), we calculated that rates of abiotic $N_2O$ production from $MnO_2$ oxidation of $NH_2OH$ would be ~500 nM $d^{-1}$, whereas measured rates were 135 nM $d^{-1}$ from denitrifying bacterial cultures obtained from the Baltic Sea (Rönner and Sörensson 1985). We acknowledge that fluctuating substrate concentrations could produce a wider range of rates, but this simple calculation suggests that abiotic $N_2O$ production could contribute significantly to $N_2O$ production in marine oxyclines.

The finding that nitroxyl (HNO), and possibly the aminoxyl radical ($H_2NO\cdot$), are intermediates in the abiotic $NH_2OH$ oxidation by Mn(III/IV) oxides suggests that alternative reactive N species may be involved in coupled biotic/abiotic interactions in the nitrogen cycle. Although

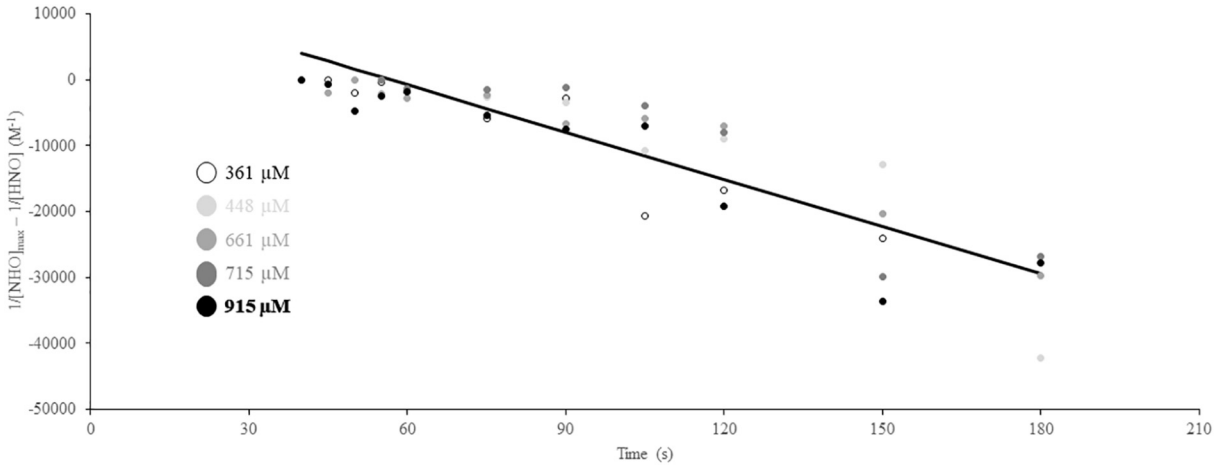


**Fig. 6.** Nitroxyl dimerization exhibits pseudo-second order characteristics. Concentrations of HNO calculated from mass balance of varied $MnO_2$ experiments in Fig. 1b-f. The second-order rate constant of HNO dimerization, $k_2$, is found to be 239 ± 93 $M^{-1}\,s^{-1}$ in the experiments. The line represents the best linear regression fit of all data sets.

HNO may also be produced as an enzymatic intermediate in the nitrogen cycle (Bykov et al. 2014; Hooper and Terry 1979; Komarov et al. 2000; Xia et al. 2000), it is commonly assumed that it remains bound to the enzyme and is rapidly converted to $NO_2^-$, $N_2O$, or $NH_4^+$ during nitrification, denitrification, and dissimilatory nitrate reduction to ammonium, respectively. Free HNO, however, is essential in nitric oxide reduction by nitric oxide synthase (Turk and Hollocher 1992), and $Mn^{2+}$ inhibits the dehydrogenation of HNO by hydroxylamine dehydrogenase (formerly hydroxylamine oxidoreductase) to produce $N_2O$ instead of $NO_2^-$ (Hooper and Terry 1979). Thus, biologically produced HNO could dimerize with HNO from abiotic $NH_2OH$ oxidation to enhance $N_2O$ production.

Although the detection limit of the $N_2O$ microsensor (1 μM) used in this study required use of higher concentrations of $NH_2OH$ than typically found in nature, the rate constants measured here should apply to lower substrate concentrations as well. The proposed rate law and the overall first order rate constant could be used in biogeochemical models to account for the proportion of $N_2O$ that is abiotically produced in a variety of environments.

## 5. Conclusions

To our knowledge, this is the first study that characterized the kinetics of $NH_2OH$ oxidation by Mn(IV) oxides in seawater at circumneutral pH. We demonstrated that the reaction is overall first order with respect to $NH_2OH$ concentrations. The reaction is rapid at circumneutral pH ($k = 0.01\ s^{-1}$), with complete oxidation occurring within minutes (half-life of ~23 s). Nitroxyl (HNO) was found to be an important intermediate in abiotic $NH_2OH$ oxidation, as mass balance considerations indicate rapid formation and disappearance of an intermediate nitrogen species, and $N_2O$ production was reduced in the presence of a HNO scavenger. Our findings suggest the potential for a novel biotic-abiotic pathway by which any $NH_2OH$ that leaks from nitrifying cells and comes in contact with reactive Mn(III/IV) oxide minerals will rapidly be oxidized to $N_2O$. The abiotic interactions between biotically produced nitrogenous intermediates and Mn oxide particles could have implications for Mn and N cycling. Future studies should focus on the distribution of ammonia-oxidizing organisms and suspended particulate Mn oxides in diverse ecosystems.

Supplementary data to this article can be found online at https://doi.org/10.1016/j.marchem.2018.03.002.

## Acknowledgments

This work was supported by the National Science Foundation Graduate Research Fellowship Program #DGE-1148903, the Georgia Tech Foundation President's Fellowship, and the Goizueta Foundation Fellowship. We would like to thank Emily Saad, Keaton Belli, Shiliang Zhao, and David Tavakoli for technical assistance, as well as Lisa Stein and Jessica Kozlowski for helpful discussions.

## References

Anderson, J., 1964. The copper-catalysed oxidation of hydroxylamine. Analyst 89 (1058), 357–362.
Anschutz, P., Dedieu, K., Desmazes, F., Chaillou, G., 2005. Speciation, oxidation state, and reactivity of particulate manganese in marine sediments. Chem. Geol. 218, 265–279.
Balistrieri, L., Murray, J., 1982. The surface chemistry of $\delta MnO_2$ in major ion seawater. Geochim. Cosmochim. Acta 46, 1041–1052.
Banerjee, S., Choudhury, U., Banerjee, R., Mukhopadhyay, S., 2002. Kinetic and mechanistic studies on the oxidation of hydroxylamine by a tri-bridged manganese (IV,IV) dimer in weakly acidic media. J. Chem. Soc. Dalton Trans. 2047–2052.
Bargar, J., Webb, S., Tebo, B., 2005. EXAFS, XANES and *in-situ* SR-XRD characterization of biogenic manganese oxides produced in seawater. Phys. Scr. T115, 888–890.
Bari, S., Amorebieta, V., Gutiérrez, M., Olabe, J., Doctorovich, F., 2010. Disproportionation of hydroxylamine by water-soluble iron(III) porphyrinate compounds. J. Inorg. Biochem. 104, 30–36.
Beman, J., Popp, B., Alford, S., 2012. Quantification of ammonia oxidation rates and ammonia-oxidizing archaea and bacteria at high resolution in the Gulf of California and the eastern tropical North Pacific Ocean. Limnol. Oceanogr. 57 (3), 711–726.
Blöthe, M., et al., 2015. Manganese-cycling microbial communities inside deep-sea manganese nodules. Environ. Sci. Technol. 49, 7692–7700.
Bonner, F., Dzelzkalns, L., Bonucci, J., 1978. Properties of nitroxyl as intermediate in the nitric oxide-hydroxylamine reaction and in trioxodinitrate decomposition. Inorg. Chem. 17 (9), 2487–2494.
Boumaiza, H., Coustel, R., Despas, C., Ruby, C., Bergaoui, L., 2018. Interaction of ammonium with birnessite: evidence of a chemical and structural transformation in alkline aqueous medium. J. Solid State Chem. 258, 543–550.
Bouskill, N., Eveillard, D., Chien, D., Jayakumar, A., Ward, B., 2012. Environmental factors determining ammoni-oxidizing organism distribution and diversity in marine environments. Environ. Microbiol. 14 (3), 714–729.
Bruland, K., Orians, K., Cowen, J., 1994. Reactive trace metals in the stratified central North Pacific. Geochem. Cosmochim. Acta 58 (15), 3171–3182.
Butler, J., Gordon, L., 1986. An improved gas chromatographic method for the measurement of hydroxylamine in marine and fresh waters. Mar. Chem. 19, 229–243.
Butler, J., Jones, R., Garber, J., Gordon, L., 1987. Seasonal distribution and turnover of reduced trace gases and hydroxylamine in Yaquina Bay, Oregon. Geochem. Cosmochim. Acta 31, 697–706.
Butler, J.H., Pequegnat, J.E., Gordon, L.I., Jones, R.D., 1988. Cycling of methane, carbon monoxide, nitrous oxide, and hydroxylamine in a meromictic, coastal lagoon. Estuar. Coast. Shelf Sci. 27, 181–203.
Bykov, D., Plog, M., Neese, F., 2014. Heme-bound nitroxyl, hydroxylamine, and ammonia ligands as intermediates in the reaction cycle of cytochrome *c* nitrite reductase: a theoretical study. J. Biol. Inorg. Chem. 19, 97–112.
Caranto, J., Lancaster, K., 2017. Nitric oxide is an obligate bacterial nitrification intermediate produced by hydroxylamine oxidoreductase. PNAS 114 (31), 8217–8222.
Clement, B., Luther, G., Tebo, B., 2009. Rapid, oxygen-dependent microbial Mn(II) oxidation kinetics at sub-micromolar oxygen concentrations in the Black Sea suboxic zone. Geochem. Cosmochim. Acta 73, 1878–1889.
Davidson, E., Kanter, D., 2014. Inventories and scenarios of nitrous oxide emissions. Environ. Res. Lett. 9. http://dx.doi.org/10.1088/1748-9326/9/10/105012/pdf.
Davies, G., Kustin, K., 1969. The stoichiometry and kinetics of manganese(III) reactions with hydroxylamine, O-methylhydroxylamine, and nitrous acid in acid perchlorate solution. Inorg. Chem. 8 (3), 484–490.
Fehling, C., Friedrichs, G., 2011. Dimerization of HNO in aqueous solution: an interplay of solvation effects, fast acid-base equilibria, and intramolecular hydrogen bonding? J. Am. Chem. Soc. 133, 17912–17922.
Feng, X., Li, W., Zhu, M., Sparks, D., 2015. Advances in the Environmental Biogeochemistry of Manganese Oxides. American Chemical Society.
Fiadeiro, M., Solórzano, L., Strickland, J., 1967. Hydroxylamine in seawater. Limnol. Oceanogr. 12 (3), 555–556.
Frear, D., Burrell, R., 1955. Spectrophotometric method for determining hydroxylamine reductase activity in higher plants. Anal. Chem. 27 (10), 1664–1665.
García-Rodledo, E., Corzo, A., Papaspyrou, S., 2014. A fast and direct spectrophotometric method for the sequential determination of nitrate and nitrite at low concentrations in small volumes. Mar. Chem. 162, 30–36.
Gebhardt, S., Walter, S., Nausch, G., Bange, H.W., 2004. Hydroxylamine ($NH_2OH$) in the Baltic Sea. Biogeosci. Discuss. Eur. Geosci. Union 1 (1), 709–724.
Heil, J., Liu, S., Vereecken, H., Brüggemann, N., 2015. Abiotic nitrous oxide production from hydroxylamine in soils and their dependence on soil properties. Soil Biol. Biochem. 84, 107–115.
Holland, K., Walker, J., 1996. Crystal structure modeling of a highly disordered potassium birnessite. Clay Clay Miner. 44 (6), 744–748.
Hooper, A., Terry, K., 1979. Hydroxylamine oxidoreductase of *Nitrosomonas* production of nitric oxide from hydroxylamine. Biochem. Biophys. Acta 571, 12–20.
Hussain, M., Stedman, G., Hughes, M., 1968. Kinetics and mechanism of the reaction between nitrous acid and hydroxylamine. Part III. The formation of hyponitrous acid. J. Chem. Soc. B 597–603.
Hynes, M., Wurm, K., Moloney, A., 1993. Reduction of the bis(pentane-2,4-dionato) diaquo manganese(III) complex by hydroxylamine and L-ascorbic acid in aqueos solution. Inorg. Chim. Acta 5–10.
IPCC, 2014. Climate change 2014: Synthesis report. In: Contribution of Working Groups I, II and III to the fifth assessment report of the Intergovernmental Panel on Climate Change. 9291691437. IPCC, Geneva, Switzerland.
Jackson, M., et al., 2009. Kinetic feasibility of nitroxyl reduction by physiological reductants and biological implications. Free Radic. Biol. Med. 47, 1130–1139.
Kartal, B., et al., 2011. Molecular mechansims of anaerobic ammonium oxidation. Nature 479, 127–132.
Komarov, A., Wink, D., Feelisch, M., Schmidt, H., 2000. Electron-paramagnetic resonance spectroscopy using *N*-methyl-D-glucamine dithiocarbamate iron cannot discriminate between nitric oxide and nitroxyl: implications for the detection of reaction products for nitric oxide synthase. Free Radic. Biol. Med. 28 (5), 739–742.
Kozlowski, J., Steiglmeier, M., Schleper, C., Klotz, M., Stein, L., 2016. Pathways and Key Intermediates Required for Obligate Aerobic Ammonia-Dependent Chemolithotrophy in Bacteria and Thaumarchaeota. ISME, pp. 1–10.
Krumbein, W., Altmann, H., 1973. A new method for the detection and enumeration of manganese oxidizing and reducing microorganisms. Helgoländer Meeresun. 25, 347–356.
Latimer, W., 1952. The Oxidation States of the Elements and their Potentials in Aqueous Solution, 2nd edn. Prentice-Hall, Englewood Cliffs.
Lin, H., Taillefert, M., 2014. Key geochemical factors regulating Mn(IV)-catalyzed anaerobic nitrification in coastal marine sediments. Geochem. Cosmochim. Acta 133, 17–33.
Liu, S., Berns, A., Vereecken, H., Wu, D., Brüggemann, N., 2017. Interactive effects of

$MnO_2$, organic matter and pH on abiotic formation of $N_2O$ from hydroxylamine in artificial soil mixtures. Sci. Rep. 7, 39590.
Löscher, C., et al., 2012. Production of oceanic nitrous oxide by ammonia-oxidizing archaea. Biogeosciences 9, 2419–2429.
Luther, G.W., 2010. The role of one- and two-electron transfer reactions in forming thermodynamically unstable intermediates as barriers in multi-Electron redox reactions. Aquat. Geochem. 16, 395–420.
Luther, G., Sundby, B., Lewis, B., Brendel, P., Silverberg, N., 1997. Interactions of manganese with the nitrogen cycle: alternative pathways to dinitrogen. Geochem. Cosmochim. Acta 61 (19), 4043–4052.
Mallik, T., 1980. Macro- and micromorphology of some manganese nodules from the Indian Ocean. Mar. Geol. 34, M45–M56.
Martí, M., Bari, S., Estrin, D., Doctorovich, F., 2005. Discrimination of nitroxyl and nitric oxide by water-soluble Mn(III) porphyrins. J. Am. Chem. Soc. 127, 4680–4684.
Moews Jr., P., Audrieth, L., 1959. The autoxidation of hydroxylalmine. J. Inorg. Nucl. Chem. 11, 242–246.
Morel, F., Rueter, J., Anderson, D., Guillard, R., 1979. Aquil: a chemically defined phytoplankton culture medium for trace metal studies. J. Phycol. 15 (2), 135–141.
Murray, J., 1974. The surface chemistry of hydrous manganese dioxide. J. Colloid Interface Sci. 46 (3), 357–371.
Nameroff, T., Balistrieri, L., Murray, J., 2002. Suboxic trace metal geochemistry in the eastern tropical North Pacific. Geochim. Coscmochim. Acta 66 (7), 1139–1158.
Neretin, L., Pohl, C., Jost, G., Leipe, T., Pollehne, F., 2003. Manganese cycling in the Gotland Deep, Baltic Sea. Mar. Chem. 82, 125–143.
Newell, S., Babbin, A., Jayakumar, A., Ward, B., 2011. Ammonia oxidation rates and nitrification in the Arabian Sea. Glob. Biogeochem. Cy 25 (4), GB4016.
Oshiki, M., Ali, M., Shinyako-Hata, K., Satoh, H., Okabe, S., 2016. Hydroxylamine-dependent anaerobic ammonium oxidation (anammox) by "*Candidatus* Brocadia sinica". Environ. Microbiol. 18 (9), 3133–3143.
Potter, R., Rossman, G., 1979. The tetravalent maganese oxides: identification, hydration, and structural relationships by infrared spectroscopy. Am. Mineral. 64, 1199–1218.
Remucal, C., Ginder-Vogel, M., 2014. A critical review of the reactivity of manganese oxides with organic contaminants. Environ. Sci. Process. Impacts 16, 1247–1266.
Riley, J., 1953. The spectrophotometric determination of ammonia in natural waters with particular reference to sea-water. Anal. Chim. Acta 9, 575–589.
Rönner, U., Sörensson, F., 1985. Denitrification rates in teh low-oxygen waters of the stratified Baltic proper. Appl. Environ. Microbiol. 50 (4), 801–806.
Salem, I., 1995. A kinetic study of the homogeneous oxidation of hydroxylamine by manganese(III)-*bis*(salicylaldimine) complexes. Transit. Met. Chem. 20, 312–315.
Samuni, Y., Goldstein, S., Dean, O., Berk, M., 2013. The chemistry and biological activities of *N*-acetylcysteine. Biochem. Biophys. Acta 1830, 4117–4129.
Santoro, A., Buchwald, C., McIlvin, M., Casciotti, K., 2011. Isotopic signature of $N_2O$ produced by marine ammonia-oxidizing archaea. Science 333, 1282–1285.
Schweiger, B., Hansen, H., Bange, H., 2007. A time series of hydroxylamine ($NH_2OH$) in the southwestern Baltic Sea. Geophys. Res. Lett. 34 (24).
Shafirovich, V., Lymar, S., 2002. Nitroxyl and its anion in aqueous solutions: spin states, protic equilibria, and reactivities toward oxygen and nitric oxide. PNAS 99 (11), 7340–7345.
Shiller, A., Gieskes, J., 1985. Particulate iron and manganese in the Santa Barbara Basin, California. Geochim. Cosmochim. Acta 49, 1239–1249.
Shiraishi, F., et al., 2016. Dense microbial community on a ferromanganese nodule from the ultra-oligotrophic South Pacific Gyre: implications for biogeochemical cycles. Earth Planet. Sci. Lett. 447, 10–20.
Soler-Jofra, A., et al., 2016. Importance of abiotic hydroxylamine conversion on nitrous oxide emissions during nitrification of reject water. Chem. Eng. J. 287, 720–726.
Solórzano, L., 1969. Determination of ammonia in natural waters by the phenolhypochlorite method. Limnol. Oceanogr. 14 (5), 799–801.
Stein, L., 2011. Surveying $N_2O$-producting pathways in bacteria. In: Klotz, M.G. (Ed.), Methods in Enzymology. Elsevier, San Diego, USA, pp. 131–152.
Strickland, J., Parsons, T., 1972. A practical handbook of seawater analysis.
Tebo, B., 1991. Manganese(II) oxidation in the suboxic zone of the Black Sea. Deep-Sea Res. 38 (2), 5883–5905.
Trefry, J., Presley, B., Keeney-Kennicutt, W., Trocine, R., 1984. Distribution and chemistry of manganese, iron, and suspended particulates in Orca Basin. Geo-Mar. Lett. 4, 125–130.
Turk, T., Hollocher, T., 1992. Oxidation of dithiothreitol during turnover of nitric oxide reductase: evidence for generation of nitroxyl with the enzyme from *Paracoccus denitrificans*. Biochem. Biophys. Res. Comm. 183 (3), 983–988.
Vajrala, N., et al., 2013. Hydroxylamine as an intermediate in ammonia oxidation by globally abundant marine archaea. PNAS 110 (3), 1006–1011.
Villalobos, M., Toner, B., Bargar, J., Sposito, G., 2003. Characterization of the manganese oxide produced by *Pseudomonas putida* strain MnB1. Geochem. Cosmochim. Acta 67 (14), 2649–2662.
Webb, S., Tebo, B., Bargar, J., 2005. Structural characterization of biogenic Mn oxides produced in seawater by the marine *bacillus* sp. strain SG-1. Am. Mineral. 90, 1342–1357.
Weiss, R., Price, B., 1980. Nitrous oxide solubility in water and seawater. Mar. Chem. 8, 347–359.
Xia, Y., Cardounel, A., Vanin, A., Zweier, J., 2000. Electron paramagnetic resonance spectroscopy with *N*-methyl-D-glucamine dithiocarbamate iron complexes distinguishes nitric oxide and nitroxyl anion in a redox-dependent manner: applications in identifying nitrogen monoxide products from nitric oxide synthase. Free Radic. Biol. Med. 29 (8), 793–797.
Yoshida, T., Alexander, M., 1964. Hydroxylamine formation by *Nitrosomonas europaea*. Can. J. Microbiol. 10 (6), 923–926.
Zhou, Y., Toupin, M., Bélanger, D., Brousse, T., Favier, F., 2006. Electrochemical preparation and characterization of birnessite-type layered manganese oxide films. J. Phys. Chem. Solids 67, 1351–1354.
Zhu-Barker, X., Cavazos, A.R., Ostrom, N.E., Horwarth, W.R., Glass, J.B., 2015. The importance of abiotic reactions for nitrous oxide production. Biogeochemistry 126, 251–267.